مجلة الدراسات التربوية والعلمية - كلية التربية - الجامعة العراقية
العدد السادس والعشرون - المجلد الأول - علوم الفيزياء - أيلول 2025 م
doi.org/10.52866/esj.2025.01.26.25

# Theoretical and Semi-Classical Models of Heavy-Ion Fusion: A Comprehensive Review of Channel Coupling and Transfer Effects Below the Coulomb Barrier

Sarah M. Obaid[1] , Zeena J. Raheem[2] , Noor Adil Mohammed[3] , Fouad A. Majeed[4]
[1]Department of Medical Physics, College of Sciences, Al-Mustaqbal University, 51001 Babylon – Hilla, Iraq.
[2]Physics Department, College of Education, Al–Iraqia University, Baghdad, Iraq
[3]Ministry of Education, Directorate General of Education Rusafa3, Baghdad, Iraq
[4]Department of Physics, College of Education for Pure Sciences, University of Babylon, Hillah, Iraq.
*Corresponding Author e-mail: sarah.mahdi@uomus.edu.iq

**Abstract**

This review highlights recent theoretical progress in predicting heavy-ion fusion events at and below the Coulomb barrier, focussing on the effects of channel coupling, nucleon transfer, and breakdown phenomena. nThe research integrates results from semi-classical and quantum mechanical approaches applied to many nuclear systems, including $^{28}Si+^{90,92}Zr$, $^{41}K+^{28}Si$, $^{6}Li+^{64}Ni$ ,$^{40}Ca+^{194}Pt$, and $^{40}Ar+^{148}Sm$. The semi-classical WKB approximation provides a first-order representation of barrier penetration while neglecting internal degrees of freedom. In contrast, quantum coupled-channels methodologies (CDCC, CCFULL) include couplings to vibrational excitations, transfer channels, and nuclear deformation, hence improving predictive accuracy at sub-barrier energies. The calculated observables fusion cross section ($\sigma_{fus}$), fusion barrier distribution ($D_{fus}$), and fusion probability ($P_{fus}$) demonstrate that including coupling effects significantly improves agreement with experimental data under the barrier. Systems that use positive Q-value neutron or proton transfer (PQNT, PQPT) show improved fusion because neck creation and nucleon exchange decrease the barrier. The results reveal that quantum mechanical calculations match experimental data better than semi-classical ones, particularly below the barrier. Above the barrier, both approaches work about the same. In general, the investigations show that coupling to inelastic, transfer, and breakup channels is necessary for accurate modelling of fusion near the barrier. These ideas are useful for studying nuclear structure, making superheavy materials, and fusion reactions in space.

**Kewwords:** Heavy-ion fusion, Coupled-channels method, Sub-barrier fusion, Quantum tunneling, Transfer and breakup coupling.

# النماذج النظرية وشبه الكلاسيكية لاندماج الأيونات الثقيلة: مراجعة شاملة لتأثيرات الاقتران بين القنوات والنقل تحت حاجز كولوم

سارة مهدي عبيد[1] ، زينه جميل رحيم[2] ، نور عادل محمد[3] ، فؤاد عطية مجيد[4]
[1] قسم الفيزياء الطبية ، كلية العلوم ، جامعة المستقبل ، بابل ، العراق
[2] قسم الفيزياء ، كلية التربية ، الجامعة العراقية ،بغداد ، العراق
[3] وزارة التربية، المديرية العامة للتربية الرصافة الثالثة، بغداد، العراق
[4] قسم الفيزياء ، كلية التربية للعلوم الصرفة ،جامعة بابل، بابل ، العراق

**مستخلص:**

تُسلّط هذه المراجعة الضوء على التقدّم النظري الأخير في التنبؤ بظواهر الاندماج النووي الثقيل عند أو دون حاجز كولوم، مع التركيز على تأثيرات اقتران القنوات، وانتقال النيوكليونات، وظواهر الانهيار. وقد دمجت الدراسة بين نتائج النماذج شبه–الكلاسيكية والكمّية، والتي طُبّقت على عدة أنظمة نووية مثل : $^{28}Si+^{90,92}Zr$, $^{41}K+^{28}Si$, $^{6}Li+^{64}Ni$ $^{40}Ca+^{194}Pt$, and $^{40}Ar+^{148}S$ يُقدّم التقريب شبه–الكلاسيكي (WKB) وصفًا من الدرجة الأولى لاختراق الحاجز، لكنه يُهمل التأثيرات الداخلية للنواة. في المقابل، توفر نماذج القنوات المترابطة الكمّية (مثل CDCC وCCFULL) إمكانية تضمين اقترانات بالاهتزازات النووية، وقنوات انتقال النيوكليونات، وتشوهات النواة، مما يُحسّن بشكل كبير من دقة التنبؤ خاصة عند الطاقات دون الحاجز. تشير القيم المحسوبة لكل من المقطع العرضي للاندماج ($\sigma_{fus}$) وتوزيع حاجز الاندماج ($D_{fus}$) و واحتمالية الاندماج ($P_{fus}$) إلى أن إدخال تأثيرات الاقتران يحسّن التوافق مع البيانات التجريبية عند الطاقات المنخفضة. كما أن الأنظمة التي تحتوي على انتقالات نيوترونية أو بروتونية ذات قيمة Q موجبة (PQNT وPQPT) تُظهر تعزيزًا واضحًا في معدلات الاندماج، نتيجة لانخفاض الحاجز بفعل تكوين العنق وتبادل النيوكليونات. وتكشف النتائج أن الحسابات الكمّية تُطابق التجارب بشكل أفضل من النماذج شبه–الكلاسيكية عند الطاقات دون الحاجز، بينما تتقارب الطريقتان في النتائج فوق الحاجز. عموما، تؤكد هذه الدراسات أن إدخال اقترانات القنوات اللاخطية، والانتقالية، يُعد ضروريًا لنمذجة دقيقة لتفاعلات الاندماج بالقرب من الحاجز. وتُعد هذه المفاهيم ذات أهمية في مجالات دراسة البنية النووية، وتكوين العناصر الفائقة الثقل، وتفاعلات الاندماج في الفضاء.

## 1. Introduction

To understand a lot of things, including how superheavy elements are made in the lab and how stars make new elements in space, we need to know how heavy-ion fusion processes work at near- and sub-barrier energy. When two nuclei collide and get over the Coulomb barrier, which is the repulsive electrical potential between them, fusion happens. This mostly happens via quantum tunnelling. The classical model says that fusion can't happen below this barrier, while quantum mechanics says that fusion can happen via barrier penetration. This makes modelling sub-barrier fusion both theoretically difficult and experimentally important.

Precise modelling of fusion cross sections requires transcending single-channel approximations. The incorporation of channel coupling to inelastic excitations, nucleon transfer, or breakdown states has been crucial for accurately replicating experimental outcomes at sub-barrier energies. The advancement of intricate methodologies, like the Coupled-Channels Formalism, the Continuum Discretised Coupled Channels (CDCC), and semi-classical approximations such as the WKB technique, has markedly enhanced the prediction capability of nuclear reaction theories.

This review looks at how both methods work with a variety of fusion systems, focussing on those with medium-mass and neutron-rich nuclei, to provide a full comparison of the two. A big part of the study focusses on how positive-Q-value neutron or proton transfer (PQNT, PQPT) and the establishment of a neck area following a collision may both make fusion more likely below the Coulomb barrier. There has been a lot of theoretical research on fusion dynamics at energy below the barrier. Early models that used the WKB approximation only looked at barrier penetration in one dimension, but they didn't have the complexity required to explain the experimental improvements seen at low energies [1, 2]. It was subsequently found that adding internal degrees of freedom and channel couplings was very important [3].

The Coupled-Channels (CC) approach became the most common way to include these kinds of effects. Dasgupta et al. [4] and Balantekin &

Takigawa [5] showed that coupling to vibrational or rotational states splits the barrier into many smaller barriers, which makes tunnelling more likely. These calculations provide results that match the observed fusion excitation functions and barrier distributions exactly. Also, neutron and proton transport pathways were quite important. Beckerman et al. [6] and Broglia et al. [7] found that positive Q-value nucleon transfer makes fusion easier by decreasing the effective barrier. Later theoretical studies employing quantum diffusion models [8] and TDHF simulations [9] backed this idea. Canto et al. [11] expanded the CDCC method, which was first created by Alder and Winther [10], to nuclear fusion. This made it possible to work with weakly bound and halo nuclei. People have used these models on systems like $^{6}Li+^{64}Ni$, $^{11}B+^{159}Tb$, and $^{6}He+^{238}U$ [12, 13]. Majeed et al. [14–16] and Musa et al. [17] have both employed quantum mechanical (CCFULL) and semi-classical (SCF) computations to look into medium-mass systems like $^{28}Si+Zr$ isotopes, $^{40}Ca+^{194}Pt$, and $^{46}Ti+^{64}Ni$. Their findings showed that quantum coupling models make the agreement with experimental cross-sections and barrier distributions below the Coulomb barrier much better, particularly when transfer and breakdown effects are taken into account.

The goal of this review is to critically examine and compare semiclassical and quantum mechanical models of heavy-ion fusion, particularly near and below the Coulomb barrier, by analyzing the effects of coupling to inelastic, transfer, and breakup channels, with the aim of evaluating their predictive accuracy and guiding future developments in nuclear reaction theory.

## 2. Theoretical Background

### 2.1 No-Coupling formalism

To get the fusion cross section, we use both semiclassical theory and a one-dimensional potential model. It is based on the idea that the relative speed of the colliding heavy ions totally determines their dynamics [18, 19]. The semiclassical model is based on the Schrödinger equation, which naturally includes the system's energy and angular momentum as well as the potential energy of radial motion. The theory also takes quantum tunnelling effects into account in a clear way. So, semiclassical theory is a really useful way to understand how quantum systems function, and it also lets us figure out the fusion cross section in a one-dimensional potential model [20].

$$\left(\frac{-\hbar^2\Delta^2}{2\mu}+V_{(r)}-E\right)\psi_{(r)}=0 \quad \text{....... ( 1 )}$$

The wave function described in Equation 1 can be determined using the time-dependent Schrödinger equation. The method is based on the assumption that the particle trajectories, derived from the traditional Rutherford trajectories, are located in a system characterized by a potential energy V(r) and a reduced mass μ. As described in [20], the real parts of the Coulomb potential and the centrifugal potential are an integral part of the method and can be used to estimate the wave function..

$$V_{(r)}=V_{c(r)}+V_{N(r)}+V_{\ell(r)} \quad \text{.......... ( 2 )}$$

An accurate treatment of classical forbidden elastic channel scattering in the coupled channel framework requires the inclusion of the imaginary part of the complex core potential to describe the important absorption process [19].

$$V_{N(r)}=U_{N(r)}-iW_{(r)} \quad \text{............... ( 3 )}$$

The significant absorption due to the interference of (ℓ) waves generated by the real and imaginary parts of the nuclear potential is studied using the wave expansion method. Semiclassical theory and previous studies show that nuclear fusion is initiated when two nuclei are close enough to cross the potential barrier and reach the inner region. Therefore, the probability of penetrating this barrier can be determined using the WKB method. These results are well documented in the literature. [18, 19, 20, 21, 22].

$$P_{fus}^{WKB}(\ell,E)=\left[1+e^{\left(2\int_{r_b^\ell}^{r_a^\ell}K_\ell(r)dr\right)}\right]^{-1} \quad \text{.. (4)}$$

Equation (4) can be expressed as where the local wave-function number is ℓ (r), limits, $r_a^\ell$ and $r_b^\ell$ are as defined by places of turning to the classical trajectory.

$$P_{fus}^{WH}(\ell,E)=\left[1+e^{\left(\frac{2\pi}{\hbar\Omega_\iota}(Vb(\ell)-E)\right)}\right]^{-1} \quad \text{..(5)}$$

Employing the Hill-Wheeler formula, the probability of penetration through the fusion barrier can be depicted, given its adjustability via a parabolic function [18].

$$P_{fus}^{WH}(\ell, E) = \left[1 + e^{\left(\frac{2\pi}{\hbar\Omega_\iota}(E - Vb(\ell))\right)}\right]^{-1} \quad .. (6)$$

The cross-sectional area of the fusion barrier can be determined using the Wenzel-Kramers-Brillouin (WKB) approximation as described in equation [22, 24]. The curvature (Ωl) and height (Vb(l)) of the barrier are crucial, while E represents the kinetic energy of the projectile hitting the target nucleus..

$$\sigma_F(E) = \frac{\pi}{k^2}\sum(2\ell + 1)\, P_{fus}^{WH}(\ell, E) \quad ..(7)$$

$$P_{fus}^{\gamma}(\ell, E) = \frac{4k}{E}\int \left|u_{\gamma\ell}(k_\gamma, r)\right|^2 W_{fus}^{\gamma}(\ell, E) \quad .. (8)$$

For the ℓ-th partial wave in the γ-channel, the radial wave function is $u_{\gamma l}(k_\gamma,r)$, and the imaginary part of the interaction potential is $W_{fus}^{\gamma}(r)$ .

**2.2. The Coupled Channels Formalism**

Nuclear collisions often induce internal excitations and various particle transfer processes in the interacting nuclei, both of which have a significant impact on the total cross section ($\sigma_{fus}$) of the fusion reaction. Due to the complex interactions between the different degrees of freedom that govern these reactions, an accurate description of nuclear fusion requires explicit consideration of the coupling between them. This is usually achieved by formulating a total wave function for the system, whose components correspond to the relevant intrinsic quantum mechanical states [25, 26]. The reaction dynamics are determined by the nuclear reaction described by the total wave function $\Psi(\vec{r},\tau)$, where r denotes the relative distance vector $\vec{r}$ and τ denotes the intrinsic coordinates of the projectile and the target. represents the collision and the corresponding intrinsic degrees of freedom of the projectile (**ξ**). For simplicity, we do not consider the internal arrangement of the target. By the Hamiltonian.

$$H = H_0(\xi) + V(\vec{r}, \xi) \quad .......... (9)$$

In this study, we neglect nuclear coupling and focus only on the projectile-target interaction, expressed as V(r,ξ) in the projectile intrinsic Hamiltonian H(ξ). Our theoretical comparison is limited to the Coulomb dipole term. Equation [27] gives the eigenvector of H (ξ).

$$H_0|\varphi_\beta\rangle = \varepsilon_\beta|\varphi_\beta\rangle \quad ........... (10)$$

The internal kinetic energy is denoted by $\epsilon\beta$. The Alder-Winther (AW) method consists of two main steps. First, the time evolution of the variable r is described by classical mechanics, resulting in a trajectory determined by the angular momentum ℓ and the collision energy E. Unlike the original AW method, which uses symmetric Rutherford trajectories, we determine the trajectory by solving the classical equations of motion with the potential $V(\vec{r})=\langle\varphi|V(\vec{r},\xi)|\varphi\rangle$, where φ is the ground state of the projectile. This key step transforms the coupled interactions into time-dependent interactions in ξ space, defined as $V_l(\xi,t)\equiv V(\vec{r_l}(t),\xi)$. Subsequently, the intrinsic dynamics is treated as a time-dependent quantum mechanical problem by expanding the wave function based on the intrinsic eigenstates [28].

$$\psi_{(\xi,r)} = \sum_\beta a_\beta(\ell,t)\varphi_\beta(\xi)e^{\frac{-i\varepsilon_\beta t}{\hbar}} \quad ...... (11)$$

Substituting this spread into the Schrödinger equation for the wave function ψ(ξ, t) yields the AW equations (see reference [29]).

$$i\hbar a_\beta(\ell,t) = \sum_\alpha a_\gamma(\ell,t)\langle\varphi_\beta|V_\ell(\xi,t)|\varphi_\beta\rangle e^{\frac{-i(\varepsilon_\beta-\varepsilon_\gamma)t}{\hbar}} \qquad (12)$$

The solution of these equations utilized the initial condition $a(\ell,t\rightarrow-\infty)=\delta_{\beta0}$, indicating that the projectile was initially in its ground state ($t\rightarrow-\infty$). The post-collision population of the angular momentum channel $\ell, P_\ell^\beta = |a_\beta(\ell,t)\ (\ell,t\rightarrow+\infty)|^2$, allows for the determination of the angle-integrated cross-section [30].

$$\sigma_\beta = \frac{\pi}{k^2}\sum_\ell(2\ell+1)P_\ell^{(\beta)} \quad ....... (13)$$

The application of this technique to fusion reactions begins with a quantum mechanical calculation of the fusion cross section using the coupled channel method. The total fusion cross section is then determined by summing the contributions of the individual channels. The development of the partial waves leads to the following equation, as shown in Ref. [31].

$$\sigma_F\& = \sum_\beta\left[\frac{\pi}{k^2}\sum_\ell(2\ell+1)P_\ell^F(\beta)\right] \quad ..(14)$$

$$P_\ell^F(\beta) = \frac{4k}{E}\int W_\beta^F(r)\left|u_{\beta\ell}(k_\beta,r)\right|^2 \quad ..(15)$$

The imaginary optical potential related to fusion in the channel uℓ(k)(r) has an absolute value |WF|. With β representing the radial wave function for the ℓ-th partial wave in the prior equation, the likelihood of fusion can be estimated using the subsequent approximation:

$$P_\ell^{(\beta)} = \mathcal{T}_\ell \left|a_\beta(\ell, t_{ca})\right|^2 \quad ........ (16)$$

The transmission factor through the barrier is denoted by $\mathcal{T}_\ell$, while $\left|a_\beta(\ell, t_{ca})\right|^2$ signifies the probability of the system [32].

**2.3. Distribution of Fusion Barrier**

$$D_{fus}(E) = \frac{d^2(E_{c.m.}\sigma_{fus})}{dE_{c.m.}^2} \quad ........ (17)$$

The fusion excitation function was derivatized to extracting the barrier distribution as the second derivative of ($E\sigma_F$) with respect to the energy [33, 34]. The point difference method was using to found the second derivative as given below. The barrier distribution is defined at energy ($E_1$ +$E_2$+$E_3$)/4[35] as

+E2+E3)/ 4 [35] as

$$\frac{d(E\sigma_F)}{dE} = 2\left(\frac{(E\sigma_F)_3-(E\sigma_F)_2}{E_3-E_2} - \frac{(E\sigma_F)_2-(E\sigma_F)_1}{E_2-E_1}\right)\left(\frac{1}{E_3-E_1}\right) \quad ........ (18)$$

where ($E\sigma_F$) are evaluated at energies ($E_i$)

ΔE The energy step used to calculate the second derivative is presented here. The statistical error $\delta_c$ associated with this second derivative at energy E was then determined using the following equation [36].

$$\delta_c = \left(\frac{E}{\Delta E^2}\right)\left[(\delta\sigma_F)_1^2 + 4(\delta\sigma_F)_2^2 + (\delta\sigma_F)_3^2\right]^{1/2} \quad ........... (19)$$

The absolute errors in the cross sections are indicated by$(E\sigma_F)_i$ Because $\delta_c$ is proportional to $\sigma_F$ for cross sections measured with a fixed percentage error, the barrier distribution diminishes at higher energies where the cross sections exhibit larger values [37-40].

**3. Results and Discussion**

This section analyses the prediction efficacy of semi-classical and quantum mechanical models for heavy-ion fusion at and under the Coulomb barrier. The WKB approximation offers a fundamental account of barrier penetration but overlooks significant nuclear structural effects, resulting in an underestimating of sub-barrier fusion. Quantum coupled-channel models (e.g., CCFULL, CDCC), which include inelastic excitations, deformation, and nucleon transfer, provide much enhanced concordance with experimental results, especially in systems including positive Q-value transfer channels. Results from systems such as $^{28}$Si+$^{90,94}$Zr, and $^{40}$Ca+$^{194}$Pt underscore the critical importance of coupling effects, which attenuate at elevated energies, leading to a convergence of both models. These results highlight the significance of channel couplings in precisely modelling fusion processes pertinent to nuclear structure, astrophysics, and the synthesis of superheavy elements.

Figure 1 shows a full comparison of the quantum mechanical coupled-channel (CC) and semi-classical fusion (SCF) models for the fusion reaction $^{28}$Si+$^{90}$Zr, using experimental data as a guide. Panel (A) shows the fusion cross section $\sigma_{\text{fus}}$ on a logarithmic scale. It is clear that models that include channel couplings (solid lines) produce much higher sub-barrier fusion cross sections than models that don't include them (dashed lines). The CC model (blue solid) is more in line with the experimental data than the SCF model (red solid), especially around and below the barrier energy $V_{\text{b}}$ = 73.66 MeV. Panel (B), which shows the fusion barrier distribution *D* fus D fus, shows strong and structured peaks in the linked scenarios. This shows that the fusion process is very sensitive to internal nuclear excitations and couplings. These characteristics are not present or are too smooth in the uncoupled simulations. This makes it further clearer how important channel couplings are for understanding the fine structure of the fusion barrier. Lastly, Panel (C) shows that the fusion probability *P* fus P fus slowly goes from almost zero to one as energy rises. Coupled calculations again do a better job of matching the experimental rise than uncoupled ones, which indicate a more sudden change. Overall, the findings show that coupling effects, especially in the quantum mechanical context, are very important for properly modelling fusion dynamics, especially in the sub-barrier zone where actual evidence is quite different from basic barrier-penetration predictions.

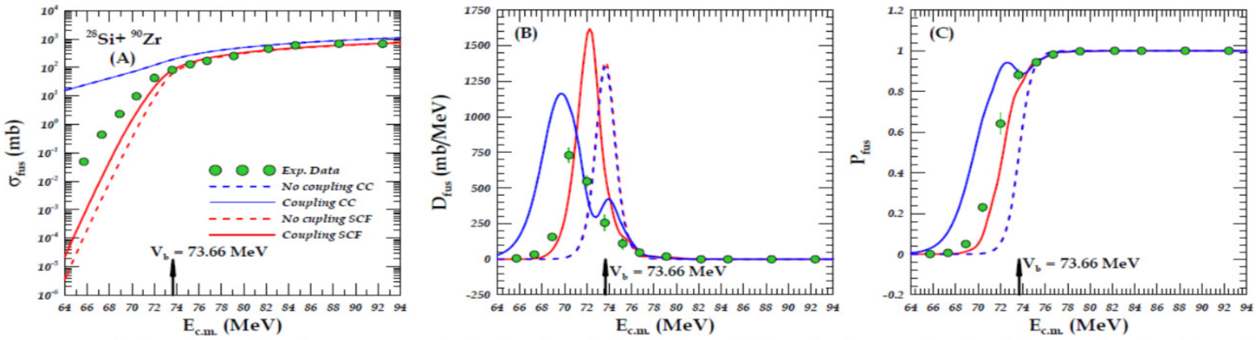


**Figure 1.** Displays the results of quantum mechanical and semi-classical calculations for the $\sigma_{fus}$ drawing (A), $D_{fus}$ drawing (B), and $P_{fus}$ drawing (C), alongside experimental data [41] for the system $^{28}$Si+$^{90}$Zr.

Figure 1: Shows the comparsion of the calculated $\sigma_{\text{fus}}$ panel (A) $D_{\text{fus}}$ panel (B) and $P_{\text{fus}}$ panel (C) for the system $^{28}$Si+$^{90}$Zr compared with the experimental data [41].

Figure 2 panels (A)–(C) depict the fusion dynamics of the $^{28}$Si+$^{92}$Zr system by juxtaposing experimental data (green circles) with theoretical predictions derived from coupled-channel (CC) and semi-classical fluctuation (SCF) models, including both coupling effects and their absence. Panel (A) illustrates the fusion cross section $\sigma$ fus σ fus as a function of the center-of-mass energy $E$ c.m. E c.m., whereby coupling effects (solid lines) markedly augment sub-barrier fusion relative to non-coupling scenarios (dashed lines), hence fitting more closely with empirical evidence. The barrier energy ($V_b$ = 72.15) MeV is provided for reference. Panel (B) displays the first derivative of the energy-weighted cross section, $D_{\text{fus}} = d(E\sigma_{\text{fus}})/dE$, which emphasises the barrier distribution. The pronounced peak around $V_b$ seen in the coupled-channel calculations is attenuated in the actual data, indicating the effects of channel couplings and potential diffuseness. Panel (C) illustrates the fusion probability \( P_{\text{fus}} \), demonstrating that coupling effects decrease the energy threshold for fusion and enhance concordance with experimental findings. The use of couplings in both CC and SCF models markedly enhances the theoretical representation of sub-barrier fusion dynamics.

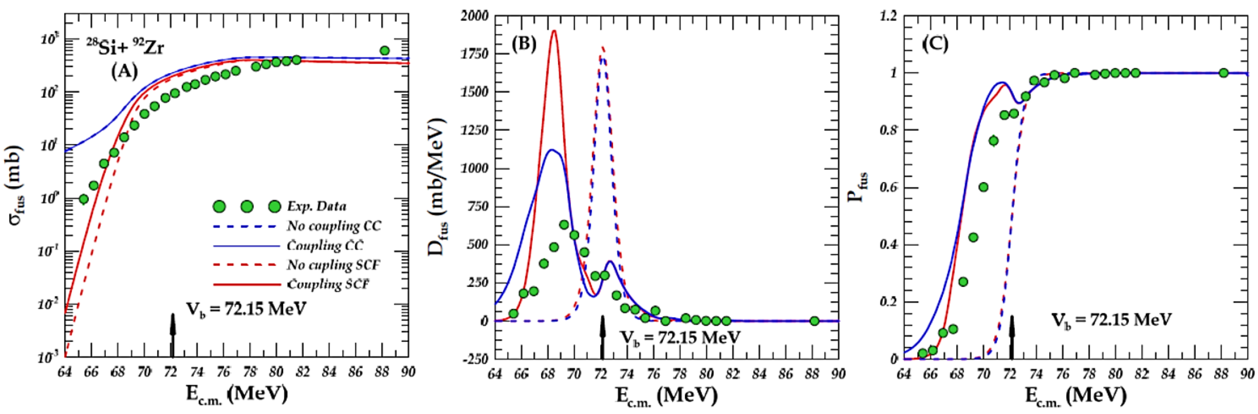


Figure 2: Shows the comparsion of the calculated $\sigma_{\text{fus}}$ panel (A) $D_{\text{fus}}$ panel (B) and $P_{\text{fus}}$ panel (C) for the system $^{28}Si+^{92}Zr$ compared with the experimental data [42].

Figure 3 illustrates a comparative examination of the fusion reaction $^{41}K+^{28}Si$ using experimental data alongside theoretical models derived from coupled-channels (CC) and semi-classical fusion (SCF) methodologies, including both coupling effects and their absence. Panel (A) illustrates the fusion cross section $\sigma_{\text{fus}}$ as a function of center-of-mass energy $E_{\text{c.m.}}$, where the experimental data (green circles) distinctly indicate a significant enhancement beneath the Coulomb barrier $V_b$ = 37.48 MeV, which is more accurately represented by the coupled SCF model (solid red line) in comparison to alternative methodologies. Panel (B) illustrates the fusion barrier distribution $D_{\text{fus}}$ obtained from the second derivative of the product ($E\sigma$), emphasising the influence of channel couplings in producing a more fragmented and structured distribution that closely corresponds with experimental characteristics. The SCF model with coupling demonstrates a better alignment with the observed peak location and width. Panel (C) illustrates the fusion probability $P_{\text{fus}}$, indicating that coupled models exhibit a distinct augmentation under the barrier, with the coupled SCF findings precisely mirroring the experimental increase and saturation pattern. The incorporation of coupling effects is crucial for accurately reflecting experimental results, and among the evaluated models, the semi-classical fusion method with coupling demonstrates the most favourable concordance across all three observables.

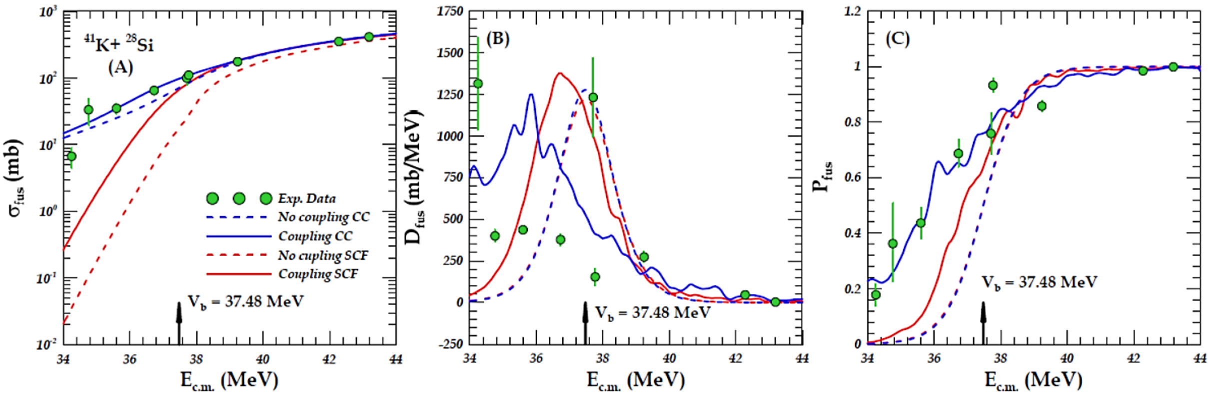


Figure 3: Shows the comparsion of the calculated $\sigma_{fus}$ panel (A) $D_{fus}$ panel (B) and $P_{fus}$ panel (C) for the system $^{41}K+^{28}Si$ compared with the experimental data [42].

Figure 4 panels (a) and (b) compare actual data with many theoretical models for the system $^{6}Li+^{64}Ni$ that use alternative coupling methods to show the fusion cross-section σ as a function of center-of-mass energy $E_{c.m.}$ for a specific nuclear reaction [44]. In both panels, the uncoupled computations (red open circles) greatly underestimate the actual results (black squares), particularly in the sub-barrier energy area. The theoretical predictions are improved by include couplings to the projectile (red dashed line) or the target (blue dashed line); nevertheless, the highest agreement is obtained over the whole energy range when both couplings are included simultaneously (solid cyan line). The significance of coupling effects in increasing the likelihood of fusion below the Coulomb barrier is well shown by the insets, which zoom into the low-energy (sub-barrier) area. These findings highlight how correct reproduction of real fusion cross-sections, especially in the barrier and sub-barrier energy regimes, requires the inclusion of both projectile and target excitations in coupled-channel computations.

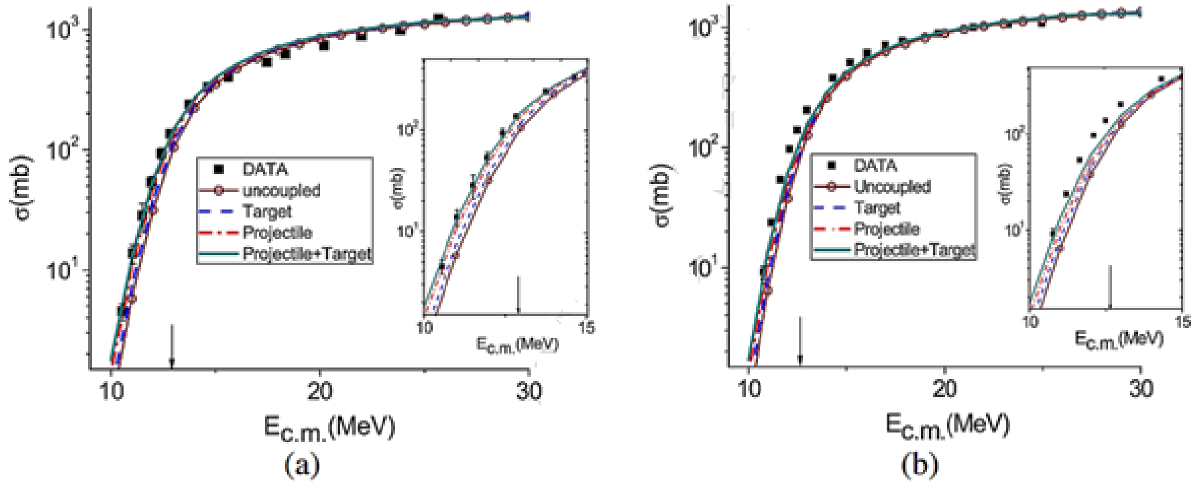


Figure 4: Compares experimental results with several coupling models to display the fusion cross sections for the $^{6}Li+^{64}Ni$ system vs center-of-mass energy. Sub-barrier fusion is underestimated in uncoupled calculations, but the fit is improved by considering couplings to the projectile or target. Incorporating both target and projectile excitations yields the best agreement, underscoring the significance of channel couplings in correctly characterising fusion below and close to the Coulomb barrier [44].

The fusion dynamics of the $^{40}Ca+^{194}Pt$ system are depicted in the figure using three important observables: (a) the fusion cross-section $\sigma$fus σ fus, (b) the fusion barrier distribution $D$fus D fus, and (c) the fusion probability $P$fus P fus, each as a function of the center-of-mass energy $E$ c.m. E c.m. The actual fusion cross-sections (green dots) in panel (a) are contrasted with theoretical predictions from a coupled-channel calculation that includes vibrational states (red), a single-channel SCF model (grey), and an expanded calculation that additionally includes two-neutron pickup (blue). The SCF model understates the data, especially in the sub-barrier area. In contrast, the agreement is much improved by coupling to vibrational and transfer channels. Panel (b) displays the distribution of fusion barriers. Unlike the abrupt peak from the SCF model, the addition of couplings results in a more organised and larger distribution that more accurately represents the observed pattern. Panel (c) displays the fusion probability, where the magenta arrow indicates the barrier energy (Vb = 174.43 MeV), where coupled-channel calculations once again closely match the experimental results. Overall, the findings highlight how important channel couplings are to precisely re-creating the fusion dynamics, especially electron transfer and vibrational excitations.

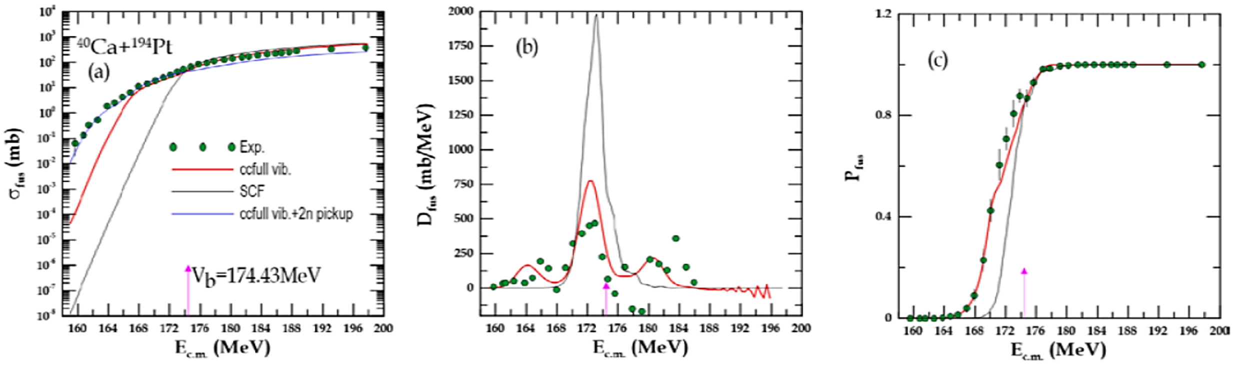


Figure 5: Shows the comparsion of the calculated $\sigma_{fus}$ panel (a) $D_{fus}$ panel (b) and $P_{fus}$ panel (c) for the system $^{40}Ca+^{194}Pt$ compared with the experimental data [42].

Figure 6 provides a detailed examination of the fusion reaction $^{40}Ar+^{148}Sm$ fusion cross section $\sigma_{fus}$, the second derivative of $E\cdot\sigma$ ($D_{fus}$), and fusion probability $P_{fus}$, all plotted against the center-of-mass energy $E_{c.m.}$. The experimental fusion cross sections (green dots) show considerable amplification at sub-barrier energies relative to the single-channel (SCF) model, indicating robust coupling effects. The coupled-channels estimate with CCFULL (red line) accurately reflects the experimental trend, particularly in the sub-barrier area. In panel (b), the distribution of the fusion barrier, $D_{fus}$, exhibits several peaks, indicating the occurrence of channel coupling, including inelastic excitations or neutron transmission. CCFULL accurately represents this structure, in contrast to the SCF model, which forecasts a single, narrow peak. The fusion probability shown in panel (c) exhibits a sharp increase near the barrier and attains saturation at elevated energies; once again, CCFULL aligns well with the data. The comparison underscores the need of including couplings to replicate the observed improvement of sub-barrier fusion and the intricate barrier structure.

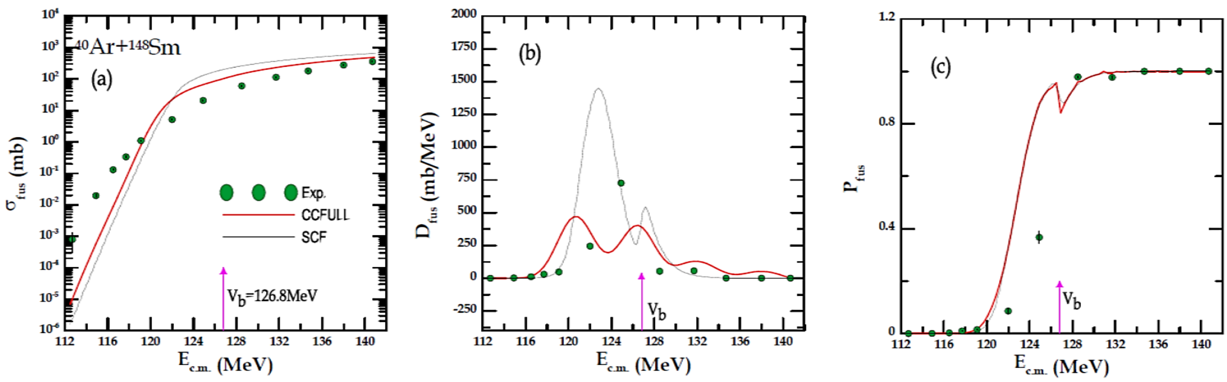


Figure 6: Shows the comparsion of the calculated $\sigma_{fus}$ panel (a) $D_{fus}$ panel (b) and $P_{fus}$ panel (c) for the system $^{40}$Ar+$^{148}$Sm compared with the experimental data [45].

## 4. Conclusion

This review critically analyses the fusion dynamics of heavy-ion systems at and below the Coulomb barrier, comparing semi-classical and quantum mechanical models, with particular emphasis on channel coupling and transfer effects. The semi-classical WKB and SCF methods, while beneficial for their conceptual clarity and classical interpretation of barrier penetration, inadequately represent experimental evidence at sub-barrier energies, when quantum effects prevail.

Quantum coupled-channel models, namely CCFULL and CDCC, provide enhanced predictive capability by including essential nuclear structural effects, including inelastic excitations, deformation, and multi-nucleon transfer, particularly those with positive Q-values (PQNT and PQPT). This addition substantially alters the effective potential barrier, resulting in increased tunnelling probabilities and fusion cross sections. The use of these models in reactions such as $^{28}$Si+$^{90,92}$Zr, $^{40}$Ca+$^{194}$Pt, and $^{41}$K+$^{28}$Si substantiates that these couplings are crucial for accurately reflecting the observed sub-barrier fusion phenomena, as shown by enhanced concordance with experimental $\sigma_{fus}$, $D_{fus}$, and $P_{fus}$ values.

The findings highlight the essential role of quantum mechanical coupling schemes in realistic models of heavy-ion fusion, especially for nuclear astrophysics, unusual nuclei, and the creation of superheavy elements. Future developments must include comprehensive microscopic analyses using time-dependent Hartree-Fock (TDHF) or density-constrained TDHF (DC-TDHF), with the methodical incorporation of breakdown and reorientation effects for weakly bound and deformed systems.

**Acknowledgments**

The author S.M. Obaid, acknowledge the financial support from Al-Mustaqbal University.

**References**

1. Balantekin, A. B., and N. Takigawa. "Quantum tunneling in nuclear fusion." Reviews of Modern Physics 70.1 (1998): 77.
2. Canto, L. F., P. R. S. Gomes, R. Donangelo, and M. S. Hussein. "Fusion and breakup of weakly bound nuclei." Physics Reports 424.1 (2006): 1–111.
3. Landowne, S., C. H. Dasso, and A. Winther. "Coupled-channels calculations in heavy-ion reactions." Nuclear Physics A 405.3 (1983): 381–396.
4. Dasgupta, M., D. J. Hinde, N. Rowley, and A. M. Stefanini. "Measuring barriers to fusion." Annual Review of Nuclear and Particle Science 48.1 (1998): 401–461.
5. Hagino, K., and N. Takigawa. "Subbarrier fusion reactions and many-particle quantum tunneling." Progress of Theoretical Physics 128.6 (2012): 1061–1106.
6. Beckerman, M., et al. "Sub-barrier fusion of heavy ions." Physical Review Letters 45.19 (1980): 1472.
7. Broglia, R. A., C. H. Dasso, S. Landowne, and A. Winther. "Fusion and surface vibrations in heavy-ion reactions." Physical Review C 27.5 (1983): 2433.
8. Zagrebaev, V. I. "Fusion enhancement due to neutron transfer in sub-barrier fusion reactions." Physical Review C 67.6 (2003): 061601.
9. Umar, A. S., and V. E. Oberacker. "Heavy-ion interaction potential deduced from density-constrained time-dependent Hartree-Fock calculation." Physical Review C 74.2 (2006): 021601.
10. Alder, K., and A. Winther. *Electromagnetic Excitations*. North-Holland, Amsterdam (1975).
11. Canto, L. F., H. D. Marta, and R. Donangelo. "Semiclassical treatment of fusion processes in collisions of weakly bound nuclei."

Physical Review C 73.3 (2006): 034608.

12. Majeed, F. A., and Y. A. Abdul-Hussien. “Coupled channel analysis of heavy-ion fusion reactions using one-dimensional barrier penetration model.” Journal of Advanced Physics 11.2 (2015).
13. Ahmed, F. K., F. A. Majeed, and T. M. Abbass. “The effect of breakup on the total fusion reaction cross section of stable bound nuclei.” Journal of Babylon University/ Pure and Applied Sciences, University of Babylon (2012).
14. Khuadher, M. A., and F. A. Majeed. “Fusion dynamics for medium-mass nuclei with transfer coupling effects.” East European Journal of Physics 3 (2023): 178–186.
15. Obaid, S. M., et al. “Coupled channel effects in the scattering of weakly bound nuclei using realistic interactions.” Journal of Physics: Conference Series 3028 (2025): 012038.
16. Majeed, F. A. “Microscopic optical model for nuclear fusion reaction studies.” International Journal of Nuclear Energy Science and Technology 11.3 (2017): 218.
17. Musa, H. J., F. A. Majeed, et al. “Semiclassical study of fusion reactions involving weakly bound projectiles.” Iraqi Journal of Physics 18.1 (2020): 84–90.
18. Canto, L. F., Donangelo, R., and Marta, H. D. “Semiclassical treatment of fusion processes in collisions of weakly bound nuclei.” Physical Review C 73 (2006): 034608.
19. Alder, K., and Winther, A. *Electromagnetic Excitations*. North-Holland: Amsterdam, The Netherlands (1975).
20. Ahmed, F. K., Majeed, F. A., and Abbass, T. M. “The effect of breakup on the total fusion reaction cross section of stable bound nuclei.” University of Babylon (2012).
21. Gomes, P. R. S., et al. “Effect of the breakup on the fusion and elastic scattering of weakly bound projectiles on Zn-64.” Physical Review C 71.3 (2005): 034608.
22. Canto, L. F., et al. “Recent developments in fusion and direct reactions with weakly bound nuclei.” Physics Reports 596 (2015): 1–86.
23. Bertulani, C. A., and Canto, L. F.

"Semiclassical calculation of Coulomb break-up of weakly-bound nuclei." Nuclear Physics A 539.1 (1992): 163–176.
24. Gomes, P. R. S., et al. "Nuclear fusion between heavy ions by the gamma-ray spectroscopy method." Nuclear Instruments and Methods in Physics Research Section A 280.2 (1989): 395.
25. Hussein, M. S., Pato, M. P., Canto, L. F., and Donangelo, R. "Real part of the polarization potential for induced fusion reactions." Physical Review C 47.5 (1993): 2398–2402.
26. Austern, N. *Direct Nuclear Reaction Theory*. Wiley, New York, NY, USA (1970).
27. Satchler, G. R. *Direct Nuclear Reactions*. Oxford University Press, Oxford, UK (1983).
28. Liang, J. F., and Signorini, C. "Fusion induced by radioactive ion beams." International Journal of Modern Physics E 14.8 (2005): 1121–1150.
29. Abramowitz, M., and Stegun, I. A. *Handbook of Mathematical Functions*. Dover Publications, New York, NY, USA (1964).
30. Gomes, P. R. S., et al. "Fusion, break-up and scattering of weakly bound nuclei." Revista Mexicana de Física 52 (2006): 2329.
31. Hussain, F. M., Majeed, F. A., and Abdul-Hussien, Y. A. "Description of coupled-channel in semiclassical treatment of heavy ion fusion reactions." Materials Science and Engineering 571 (2019): 012113.
32. Baby, L. T., et al. "Fusion dynamics in weakly bound systems." Physical Review C 62.1 (2000): 01460.
33. Hussain, F. M., and Majeed, F. A. "Quantum mechanical calculations of fusion reactions induced by multi-neutron halo systems below and above Coulomb barrier." International Journal of Nuclear Energy Science and Technology 15.1 (2021): 23–35.
34. Khuadher, M. A., and Majeed, F. A. "Probing the effects of nucleon transfer reactions on fusion cross sections and barrier distributions in Si, S, Cl+Zr systems at near-barrier energies." AIP Conference Proceedings 3169.1 (2025).
35. Abdul-Hamza, E. D., Majeed, F. A., and Hussain, F. M. "Effect of coupled and breakup channels in total and elastic scattering of weakly

bound nuclei for 6,7Li+64Zn and 6He+120Sn systems." AIP Conference Proceedings 2414.1 (2023).

36. Mehemed, M. S., Obaid, S. M., and Majeed, F. A. "Coupled channels calculation of fusion reaction for selected medium systems." International Journal of Nuclear Energy Science and Technology 14.2 (2020).
37. Nunes, F. M., and Thompson, I. J. "Multistep effects in sub-Coulomb breakup." Physical Review C 59.5 (1999): 2652.
38. Wolski, R., et al. "Sub-barrier fusion of 6He with 206Pb." European Physical Journal A 47 (2011): 111.
39. Trotta, M., et al. "Large enhancement of the sub-barrier fusion probability for a halo nucleus." Physical Review Letters 84.11 (2000): 2342.
40. Asher, B. W., et al. "Experimental study of the 17F+12C fusion reaction and its implications for fusion of proton-halo systems." Physical Review C 103.4 (2021): 044615.
41. Kalkal, S., et al. "Channel coupling effects on the fusion excitation functions for Si28+Zr90,94 in sub- and near-barrier regions." Physical Review C 81.4 (2010): 044610.
42. Newton, J. O., et al. "Experimental barrier distributions for the fusion of 12C, 16O, 28Si, and 35Cl with 92Zr and coupled-channels analyses." Physical Review C 64.6 (2001): 064608.
43. Johnstone, J. E. "The influence of shell structure on near-barrier fusion of neutron-rich nuclei." PhD thesis, Indiana University (2022).
44. Rani, N., Singh, P., Singh, M., Kumar, R., Kumar, R., and Kharab, R. "Influence of coupling of excited states and of deuteron transfer on fusion reactions induced by 6, 7Li on 64Ni, 152Sm and 209Bi targets." Nuclear Physics A 990 (2019): 149–161.
45. Reisdorf, F., et al. "Fusion and evaporation residue formation in heavy systems." Nuclear Physics A 438.1 (1985): 212–252.